Macromolecular Research

Article

DOI 10.1007/s13233-017-5113-x

www.springer.com/13233 pISSN 1598-5032 eISSN 2092-7673

Effects of Processing Methods on the Electrical Conductivity, Electromagnetic Parameters, and EMI Shielding Effectiveness of Polypropylene/Nickel-Coated Carbon Fiber Composites

Seung Hwan Lee[1,2]
Jae Young Kim[1]
Chong Min Koo*[,2,3]
Woo Nyon Kim*[,1]

[1] Department of Chemical and Biological Engineering, Korea University, Anam-ro 145, Seongbuk-gu, Seoul 02841, Korea
[2] Materials Architercturing Research Center, Korea Institute of Science and Technology, 5, Hwarang-ro 14-gil, Seongbuk-gu, Seoul 02792, Korea
[3] KU-KIST Graduate School of Science and Technology, Korea University, Anam-ro 145, Seongbuk-gu, Seoul 02841, Korea

Received April 6, 2017 / Revised May 16, 2017 / Accepted May 22, 2017

Abstract: The effects of composite preparation methods on the electrical conductivities, the electromagnetic parameters and the electromagnetic interference (EMI) shielding effectiveness of polypropylene (PP)/nickel-coated carbon fiber (CF) composites were investigated. The composites were prepared by injection molding machine, internal mixer, and screw extruder. The electrical properties results showed the PP/CF (70/30, wt%) composites prepared by injection molding demonstrated the highest electrical conductivity and EMI shielding effectiveness, which were 1.75×10^{1} S/cm and 48.4 dB at the frequency of 10 GHz, respectively. These results seem mainly due to the increased CF length when the PP/CF composite was prepared by injection molding, which was advantageous in forming a conductive network of the composite. The results of the electromagnetic parameters of the PP/CF composites showed that the increased electrical conductivity of the composite prepared by injection molding was mainly due to the increased dielectric constants (ε' and ε'') of the PP/CF composite. This enhancement in dielectric constants seems related to the percolation at a lower concentration of the CF, which was affected by the increased CF length of the composite prepared by injection molding process. The results of dielectric loss and magnetic loss factors of the PP/CF composite showed that the major electromagnetic absorbing mechanism was dielectric loss, namely dipole polarization and interface polarization between filler and matrix, which resulted in improved EMI absorption values. The total EMI shielding effectiveness (SE_T) of the PP/CF composite comprised 85.1% EMI shielding effectiveness by absorption (SE_A), and 14.9% EMI shielding effectiveness by reflection (SE_R), which suggests that the EMI shielding was predominantly by the absorbing mechanism of the incident electromagnetic wave.

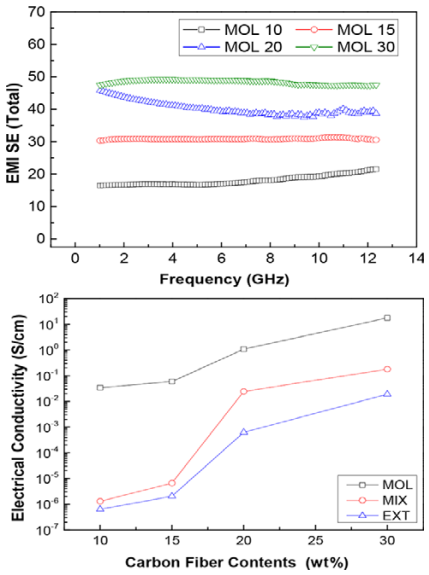

Keywords: polymer composite, electrical conductivity, EMI shielding effectiveness, carbon fiber.

1. Introduction

With the advancement of electronic devices and telecommunication equipment, electromagnetic interference (EMI) has become an important issue, as it can cause serious malfunctions of electronic componentry and harmful effects on human beings.[1-3] Metals (*e.g.*, silver and copper) have been the most commonly used materials for EMI shielding fields, because they have excellent electrical conductivity, which is required to achieve high EMI shielding effectiveness. However, metals have the inconvenience of high density, corrosion and limited processing diversity.

To alleviate this problem, various strategies have been undertaken by researchers, especially focusing on the composites of polymer/conductive fillers, such as carbon fiber,[4-6] carbon nanotube,[7-14] carbon black,[15] and graphene.[16-18] One of the major aims has been to attain an electrical conductivity that is as high as possible, with minimal use of conductive filler. Improvement in electrical conductivity has often been studied by enhancing the dispersion status of the fillers,[19-21] doping or plating,[22,23] and fabricating the structure of composites.[24] However, high electrical conductivity to achieve high EMI shielding effectiveness also increases reflection of the electromagnetic wave,[25] which in some cases might result in damage to nearby devices. For example, if a material has 10 decibel (dB) of reflection, this means that 90% of the incident wave energy will be reflected at the surface.

Recently, studies of microwave absorbers have gained a lot

Acknowledgments: This research was supported by the LG Hausys and the Brain Korea 21 Plus Program.

***Corresponding Authors:** Woo Nyon Kim (kimwn@korea.ac.kr)
Chong Min Koo (koo@kist.re.kr)

of attention, as a microwave absorber is a material that can effectively absorb electromagnetic waves, and suppress the reflection.[8] In order to have a high absorption property, dielectric material (*e.g.*, TiO_2, SiO_2, SnO_2), magnetic material (*e.g.*, Ni, Fe_2O_3, Fe_3O_4), and their combinations have been extensively studied.[25-32] For example, Zhao *et al.*[25] reported Ni shell SnO_2 core structure, which yielded reflection loss values of -29.7 dB at 1.8 mm, when composites contained 50 wt% of conductive filler. In the studies of polyethersulfone/carbon nanotube composites, Abbas and Kim[7] have reported the EMI shielding effectiveness of 35 dB in the X-band at a low thickness of 0.5 mm.

Previously, we have investigated the synergistic effects of nickel-coated carbon fiber (CF) with other conductive fillers on the electrical conductivity and EMI shielding effectiveness of the polymer/hybrid conductive filler composites.[33-35] It has been reported that nickel-coated CF is advantageous in forming electrical networks, since CF has a high length-to-diameter ratio, and nickel possesses high EMI wave absorption properties.[36-38] However, the shielding mechanism and the electromagnetic parameters of the nickel-coated CF itself have not been fully clarified, which are crucial in developing the microwave absorber.

The purpose of the present study is to investigate the EMI shielding effectiveness and electromagnetic parameters, such as the dielectric constants (ε' and ε'') and magnetic parameters (μ' and μ''), of the polypropylene (PP)/CF composite, in relation to the composite preparation methods. It is suggested that nickel possesses magnetic properties, and carbon fiber plays an important role in dielectric loss, therefore yielding synergistic effect on the EMI absorption properties.[38] Also, from the industrial point of view, it is important to reveal the effect of composite preparation methods on the electrical conductivity, electromagnetic parameters, and EMI shielding effectiveness of the polymer/conductive filler composites. To the best of our knowledge, there have been few studies that have simultaneously reported on the investigation of EMI shielding effectiveness and electromagnetic parameters.[7] PP is an important industrial material since it has many applications and the capability of being conductive or reinforced with various types of fillers. In this study, we report the relation between electromagnetic parameters and EMI shielding effectiveness of the PP/nickel-coated CF composites, when the samples were prepared by injection molding, internal mixer and screw extrusion.

2. Experimental

2.1. Materials

PP (grade: BJ 700) was supplied by Hanwha Total Ltd. (Seoul, Korea). The weight average molecular weight of PP was 36,400 g/mol. The density of the PP was 0.91 g/cm^3. Nickel-coated carbon fiber (CF) and PP/nickel-coated CF (70/30, wt%) master batch were obtained by Bullsone Material Co. Ltd. (Seoul, Korea). The diameter of the CF was about 7.0 μm. The CF used in the preparation of nickel-coated CF was supplied by Toray (grade T-700). The nickel was coated with a thickness of 300 nm on the surface of the CF, to enhance the electrical conductivity of the CF.[38] The density, and electrical and thermal conductivities of the nickel-coated CF were 2.8 g/cm^3, and 8.2×10^3 S/cm and 450 W/mK, respectively.

2.2. Preparation of composite samples

PP/CF composite samples were prepared by two steps. First, the master batch of the PP/CF (70/30, wt%) was prepared by pultrusion process at 210 °C. Secondly, the PP/CF (70/30) master batch was processed by injection molding machine, internal mixer, and screw extruder, to investigate the effects of processing method on the electromagnetic properties of the PP/CF composites. For the injection molding processing, an injection molding machine with an 18 mm screw of 20:1 length-to-diameter ratio was used. The injection molding temperature ranged from 180 to 200 °C, with a screw speed of 200 rpm, and plasticizing time of 3.62 s. The samples of PP/CF composite were also processed using internal mixer (Thermo Scientific, Model Haake Polydrive R600, Waltham, Mass., USA). The screw speed and mixing time were 80 rpm and 5 min, respectively. For the PP/CF composite samples processed by screw extrusion, a co-rotating twin-screw extruder (BauTek, Model D19, Seoul, Korea) was used. The extrusion temperature ranged from 180 to 200 °C, and the screw speed was 80 rpm. Table 1 shows the compositions and sample preparation methods of the PP/CF composites. For the samples of PP/CF (90/10, wt%) prepared using injection molding machine, internal mixing, and screw extrusion, the sample codes were listed as MOL 10, MIX 10, and EXT 10, respectively (Table 1).

2.3. Morphology

The morphology of the composites was examined by field emission scanning electron microscopy (SEM) (FEI Company model Inspect F50, Oregon, USA) at 15.0 kV. The samples were coated with platinum. To investigate the fiber length of the composite, xylene was used as a solvent to dissolve the polymers by Soxhlet extractor, and the fiber length was then measured using a microscope.

2.4. Electrical properties

Electrical conductivities of the PP/CF composites were measured

Table 1. Sample preparation methods and compositions of the polypropylene (PP)/nickel-coated carbon fiber (CF) composites

Preparation methods	PP (wt%)	CF (wt%)	Sample code
Injection molding	90	10	MOL 10
	85	15	MOL 15
	80	20	MOL 20
	70	30	MOL 30
Internal mixing	90	10	MIX 10
	85	15	MIX 15
	80	20	MIX 20
	70	30	MIX 30
Screw extrusion	90	10	EXT 10
	85	15	EXT 15
	80	20	EXT 20
	70	30	EXT 30

by linear four-pin probe (MCP-TP06P PSP) with a Loresta-GP Low resistivity meter (Model MCP-T610, Mitsubishi Chemical, Tokyo, Japan). The inter-pin distance of the probe was 1.5 mm, and the limit voltage was set as 90 V. The composites were pressed and cut into rectangular shape (25×12×0.2 mm^3). The EMI shielding effectiveness and electromagnetic parameters, such as ε' (dielectric constant: real part), ε'' (dielectric constant: imaginary part), μ' (magnetic permeability: real part), and μ'' (magnetic permeability: imaginary part), of the PP/CF composites were measured by 2-port network analyzer (Model ENA5071C, Agilent Technologies, Santa Clara, CA, USA) with coaxial holder. The frequency range of measurement was 1.0 to 12.4 GHz. Before measurement, calibration process was performed on port 1 and port 2 using open, short, and load kit. For the measurements of EMI shielding effectiveness and electromagnetic parameters, composite samples were pressed into toroidal-shape mold (φ_{in}=3.0 mm, φ_{out}=7.0 mm), with thickness of 2 mm at 210 °C. The absorption part of EMI shielding effectiveness (SE_A) was calculated using scattering parameters (S_{11}, S_{21}) by Eq. (1), as follows:[16,38,39]

$$SE_A = 10 \log((1-|S_{11}|^2)/|S_{21}|^2) \quad (1)$$

where S_{11} and S_{21} are the scattering parameters that represent the surface reflection coefficients at both ends of the sample (S_{11}, S_{22}), and the transmission coefficients of the forward and reverse transmission (S_{12}, S_{21}), respectively.

3. Results and discussion

3.1. Morphology of the PP/CF composites

Figure 1(a)-(c) shows SEM imagery of the cross-sectional surfaces of PP/CF (90/10, wt%) composites prepared by MOL 10, MIX 10, and EXT 10, respectively. These figures show that carbon fibers were randomly oriented in the polymer matrix. However, it is hard to observe the length and nickel-coated surfaces of the CF, as most of the CF is embedded in the polymer matrix. Figure 2(a)-(c) shows the CF after the PP matrix was dissolved, using xylene as a solvent. The insets of Figure 2(a)-(c) show magnified SEM imagery of the CF after each process of the PP/CF (90/10, wt%) composites. In the case of the injection molding process (Figure 2(a)), the average CF length was found to be 884 μm, and showed the least surface damage among the three different processes. On the other hand, composite prepared by the screw extruder (Figure 2(c)) showed the shortest CF length, which was found to be 407 μm. Furthermore, some of the nickel coating on the CF surface was exfoliated, as the inset of Figure 2(c) shows. In the case of composite prepared by the internal mixer (Figure 2(b)), the average CF length was 613 μm, and suffered moderate surface damage to the CF. This might be attributed to the different shear stress applied to the CF. To be more specific, the screw extruder has high shear stress, leading to increased collision between filler-filler and filler-matrix; whereas in the injection molding machine, carbon fiber undergoes minimum shear stress and short residence time.

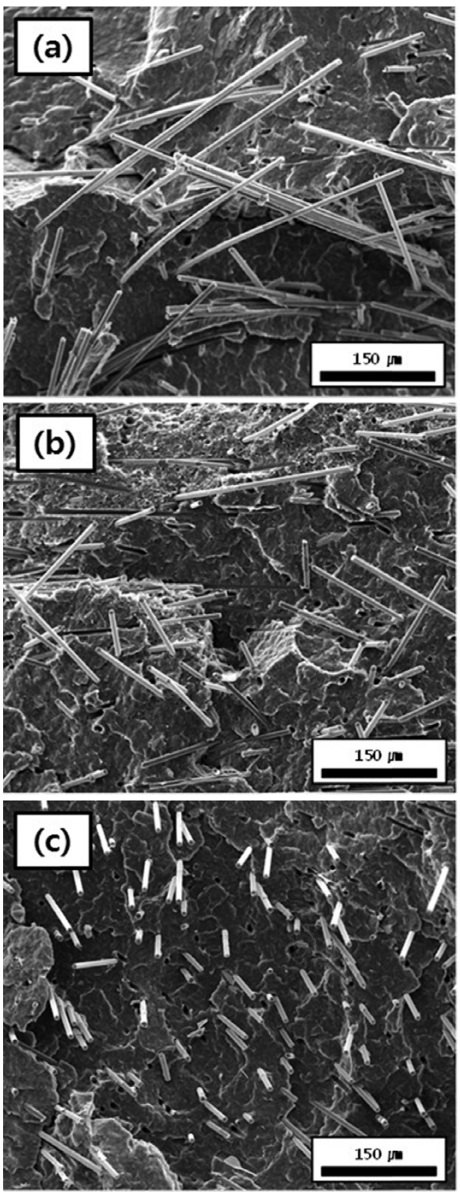

Figure 1. Scanning electron micrography images of the PP/CF (90/10, wt%) composites with sample preparation methods: (a) Injection molding, (b) internal mixing, and (c) screw extrusion.

3.2. Electrical conductivities of PP/CF composites

Figure 3 shows the electrical conductivities of the PP/CF composites prepared by injection molding, internal mixer, and screw extrusion. Figure 3 shows that the composites prepared by injection molding displayed the highest electrical conductivity, which was 1.75×10^{1} S/cm when the CF content was 30 wt%. On the other hand, the composites prepared by internal mixer and screw extruder showed 1.78×10^{-1} and 1.90×10^{-2} S/cm, respectively, when the CF content was 30 wt%. High aspect ratio of conducting filler is maybe easy to obtain filler-filler network structure.[40] From the above electrical conductivity results, it is suggested that the composites prepared by injection molding have much lower percolation thresholds and higher electrical conductivities, compared to the composites prepared by internal mixer and screw extruder, which is in good agreement with

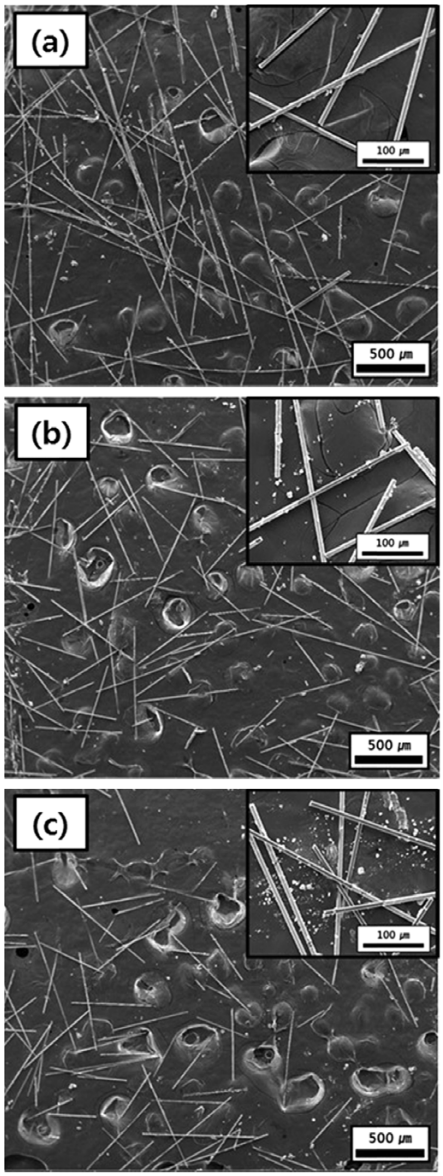

Figure 2. Scanning electron micrographs of the CF after different processing methods: (a) injection molding, (b) internal mixing, and (c) screw extrusion. The magnified SEM images of the CF are shown in the inset.

the morphological results shown in Figure 1. As discussed in Figure 2, the PP/CF composite prepared by injection molding showed the longest fiber length (884 μm), compared to those of the composites prepared by internal mixer (613 μm) and screw extrusion (407 μm), which is advantageous in forming conductive networks for the composite prepared by injection molding. Therefore, the highest electrical conductivity was observed when the composite was prepared injection molding because of the longest fiber length compared to those of the composites prepared by internal mixer and screw extrusion.

From Figure 3, the rapid increase in electrical conductivity of the PP/CF composites prepared by internal mixer and screw extrusion was observed when the carbon fiber content increased from 15 to 20 wt%. This is maybe due to that the filler-filler network is increased suddenly when the amount of carbon fiber is increased to 20 wt%. From Figure 4(c), we can see the increased filler-filler network structure of the PP/CF (80/20, wt%) com-

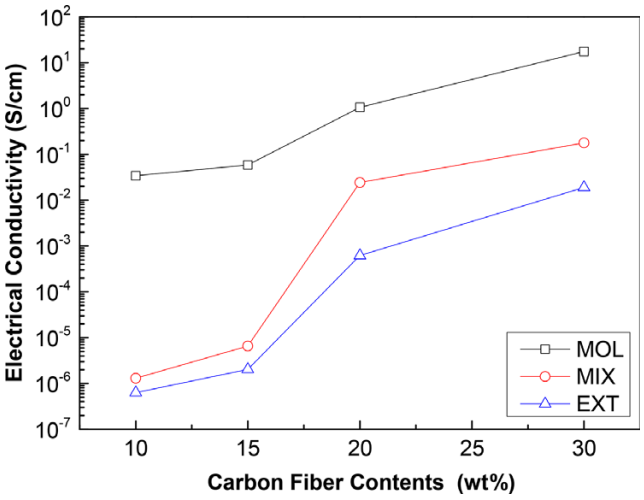

Figure 3. Electrical conductivity of the PP/CF composites with sample preparation methods: (□) Injection molding, (○) internal mixing, and (△) screw extrusion.

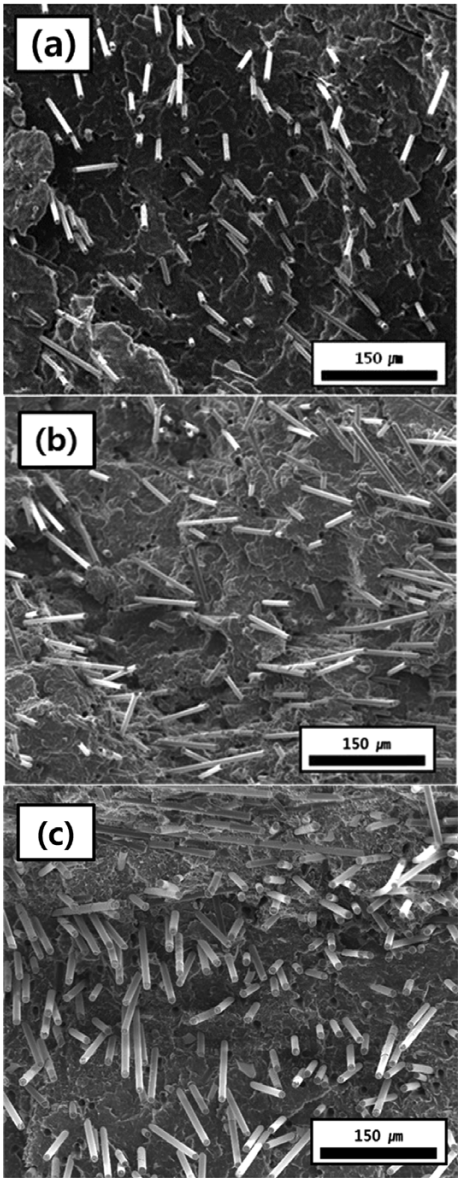

Figure 4. Scanning electron micrography images of PP/CF composites with CF contents (wt%): (a) 90/10, (b) 85/15, and (c) 80/20.

posite prepared by screw extrusion.

3.3. Electromagnetic parameters of the PP/CF composites

In an electromagnetic shielding field, the shielding performance is closely related to the electromagnetic parameters, such as the complex relative permittivity ($\varepsilon_r=\varepsilon'-j\varepsilon''$), and complex relative permeability ($\mu_r=\mu'-j\mu''$). These parameters are also important in revealing the absorption mechanism. To be more specific, the real part of the permittivity and permeability shows the storage capability of electromagnetic wave energy, whereas the imaginary part of the permittivity and permeability shows the loss capability of electromagnetic wave energy.[41] Figure 5(a)-(c) shows the electromagnetic parameters (ε', ε'', μ', and μ'') of the PP/CF (90/10, wt%) composites prepared by MOL 10, MIX 10, and EXT 10, respectively. Figure 5 shows that the dielectric constants of the real part (ε', energy storage) of the PP/CF (90/10, wt%) composite prepared by injection molding showed in the range of 17.2 to 33.3, which were higher values than those of the PP/CF (90/10, wt%) composite prepared by internal mixer and screw extrusion, which ranged from 9.5 to 15.0. Meanwhile, the dielectric constants of the imaginary part (ε'', energy loss) of the PP/CF (90/10, wt%) composite prepared by injection molding showed in the range of 6.3 to 18.1, which values were also higher than those of the PP/CF (90/10, wt%) composite prepared by internal mixer and PP/CF (90/10, wt%) composite prepared by screw extrusion in most of the frequency range. This enhanced permittivity may be related to the percolation at a lower concentration CF of the PP/CF composites.

Previously, Pötschke *et al.*[42] investigated the effect of the percolation structure on the dielectric property of polycarbonate/multiwalled carbon nanotube (1.4 wt%) composite. They reported that when the composite had a percolated structure, the permittivity abruptly increased in the low frequency range. Our electrical conductivity results shown in Figure 3 are closely related to the permittivity data (ε' and ε'') shown in Figure 4, and the electrical conductivity data seems also to be affected by the morphological behavior shown in Figure 1. In the case of magnetic parameters such as μ' and μ'' shown in Figure 5(a)-(c), all the composites showed close to 1.0 for the real part (μ'), while the imaginary part (μ'') is relatively low compared to μ' in the measured frequency range. It has been reported that the permeability of magnetic material is rapidly decreased after the resonance frequency, which is termed Snoek's limit.[43]

The results of the electromagnetic parameters (ε', ε'', μ', and μ'') of the PP/CF composites suggest that the increased electrical conductivity of the PP/CF composites prepared by injection molding was mainly due to the increased dielectric constants of the real part (ε') and the imaginary part (ε'') of the PP/CF composite. This enhanced permittivity ($\varepsilon_r=\varepsilon'-j\varepsilon''$) may be related to

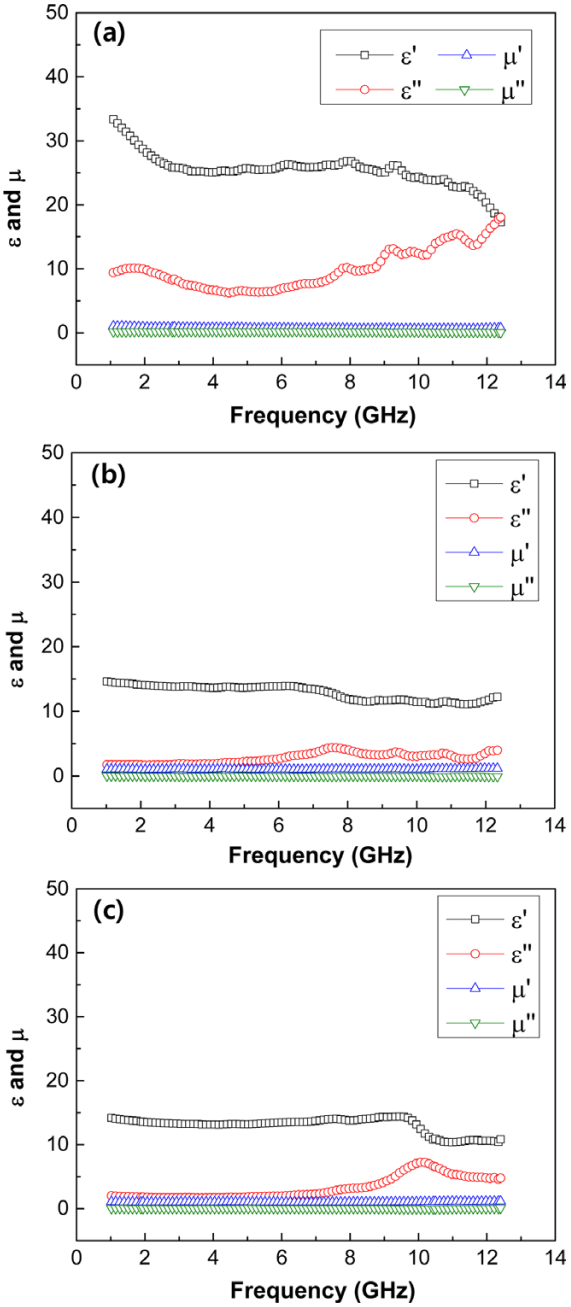

Figure 5. Electromagnetic parameters of the dielectric constants (ε', ε'') and magnetic permeability (μ', μ'') of the PP/CF composites with sample preparation methods: (a) Injection molding, (b) internal mixing, and (c) screw extrusion.

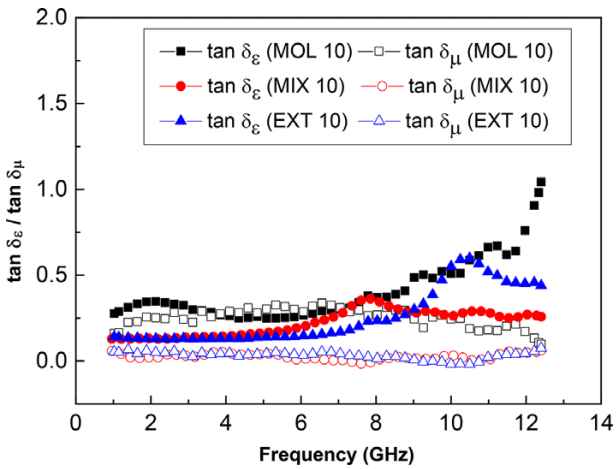

Figure 6. Dielectric loss factor (tan δ_ε) and magnetic loss factor (tan δ_μ) of the PP/CF (90/10, wt%) composites with sample preparation methods: (■, □) injection molding, (●, ○) Internal mixing, and (▲, △) screw extrusion.

the percolation at a lower concentration of the CF, which was affected by the increased CF length of the composite prepared by injection molding.

Figure 6 shows the dielectric loss factor (tan $\delta_\varepsilon=\varepsilon''/\varepsilon'$) and magnetic loss factor (tan $\delta_\mu=\mu''/\mu'$) of the PP/CF (90/10, wt%) composites prepared by injection molding, internal mixer, and screw extrusion, which were calculated in order to investigate the electromagnetic wave absorbing mechanism. The figure shows that tan δ_ε is larger than tan δ_μ in most of the frequency range for all of the composites, which suggests that the major electromagnetic wave absorbing mechanism is dielectric loss, such as dipole polarization and interface polarization between the filler and matrix.[44]

3.4. EMI shielding effectiveness of PP/CF composites

The EMI shielding effectiveness (SE) is defined by the logarithmic ratio of the incident and transmitted power, as in Eq. (2):[38,39,45]

$$\text{EMI SE (dB)} = -10 \log(P_T/P_I) \quad (2)$$

where, P_I and P_T are the incident and transmitted power of the electromagnetic wave, respectively. According to the electromagnetic wave theory, the EMI shielding effectiveness can be expressed in the far field region by Eqs. (3) and (4):[16,38,39,45]

$$SE_T\ (dB) = SE_R + SE_A \quad (3)$$
$$SE_R\ (dB) = 39.5 + 10 \log(\sigma/(2\pi\mu f)) \quad (4)$$

where, SE_T is the total part of the EMI shielding effectiveness, SE_R is the EMI shielding due to reflection, SE_A is the EMI shielding due to the absorption, σ is the electrical conductivity, f is the frequency, and t is the thickness of composite.

Figure 7(a)-(c) shows the total part of the EMI shielding effectiveness (SE_T) of the PP/CF composites prepared by injection molding, internal mixer and screw extrusion, respectively. The figures show that the SE_T of the composites increased when the amount of CF is increased. Figure 7(a) shows that for the PP/CF (70/30, wt%) composite prepared by injection molding, the EMI shielding effectiveness was observed to be 48.4 dB at the frequency of 10 GHz, which means that according to Eq. (2), 99.998 % of the EMI incident wave is shielded. Figure 7(b) and (c) shows that for the PP/CF (70/30, wt%) composites prepared by internal mixer and screw extrusion, the EMI shielding effectiveness showed lower values compared to that of the composite prepared by injection molding, which values were 28.1 dB and 22.0 dB at the frequency of 10 GHz, respectively. These results seem mainly to be attributable to the different CF length of the composites originating from different processing methods. As discussed in Figure 2, the PP/CF composite prepared by injection molding showed the longest fiber length (884 μm), compared to those of the composites prepared by internal mixer (613 μm) and screw extrusion (407 μm), which is advantageous in forming conductive networks for the composite prepared by injection molding. Therefore, the highest EMI shielding effectiveness was observed when the composite was prepared injection molding because of the longest fiber length compared to those of the composites prepared by internal mixer and screw extrusion.

Figure 8(a)-(c) shows the absorption part of the EMI shielding effectiveness (SE_A) of the composites prepared by injection molding, internal mixer, and screw extrusion, respectively. The figures show that when the amount of CF is increased, the SE_A of the composites increased. The SE_A was calculated using the scattering parameters (S_{11}, S_{12}, S_{21}, and S_{22}) of the composite shown in Eq. (1). Figure 8 shows that the SE_A values of the PP/CF (70/30, wt%) composites prepared by injection molding, internal mixer, and screw extrusion are observed to be 39.6, 24.3, and 18.8 dB, respectively, at the frequency of 10 GHz. Figures 6 and 7 show that in terms of the EMI shielding effectiveness of the composites, the value of SE_A is predominant, compared

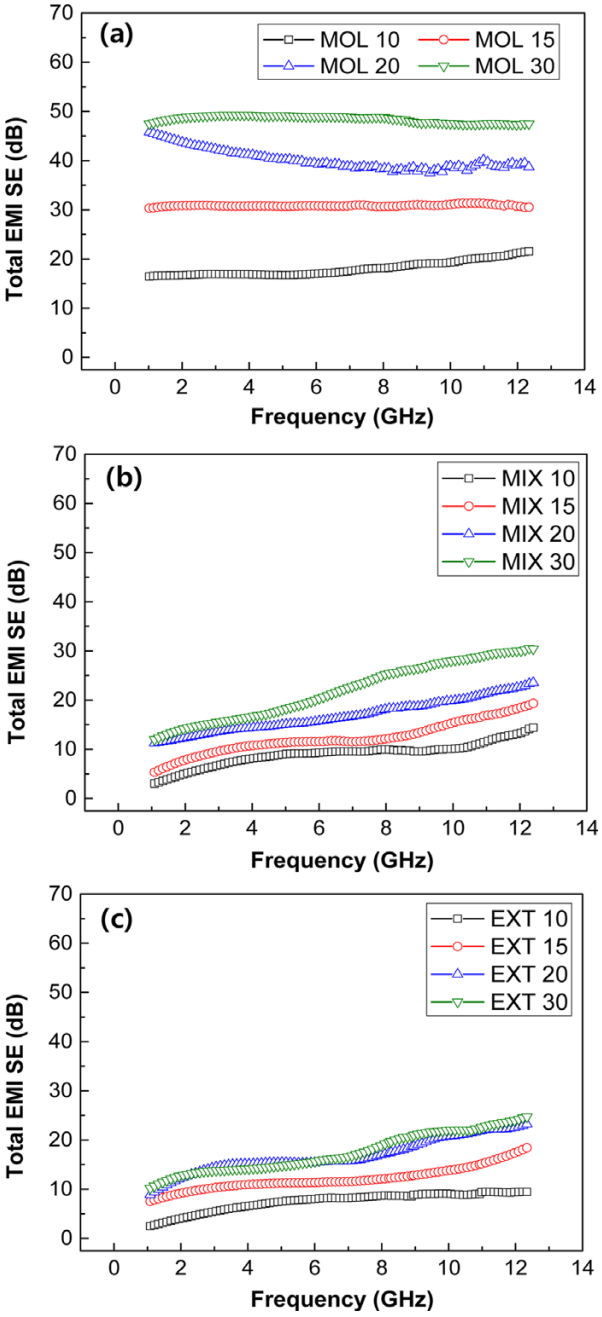

Figure 7. Total part of the EMI shielding effectiveness (SE_T) of the PP/CF composites with frequency and CF contents. Samples were prepared by different processing methods: (a) Injection molding, (b) internal mixing, and (c) screw extrusion.

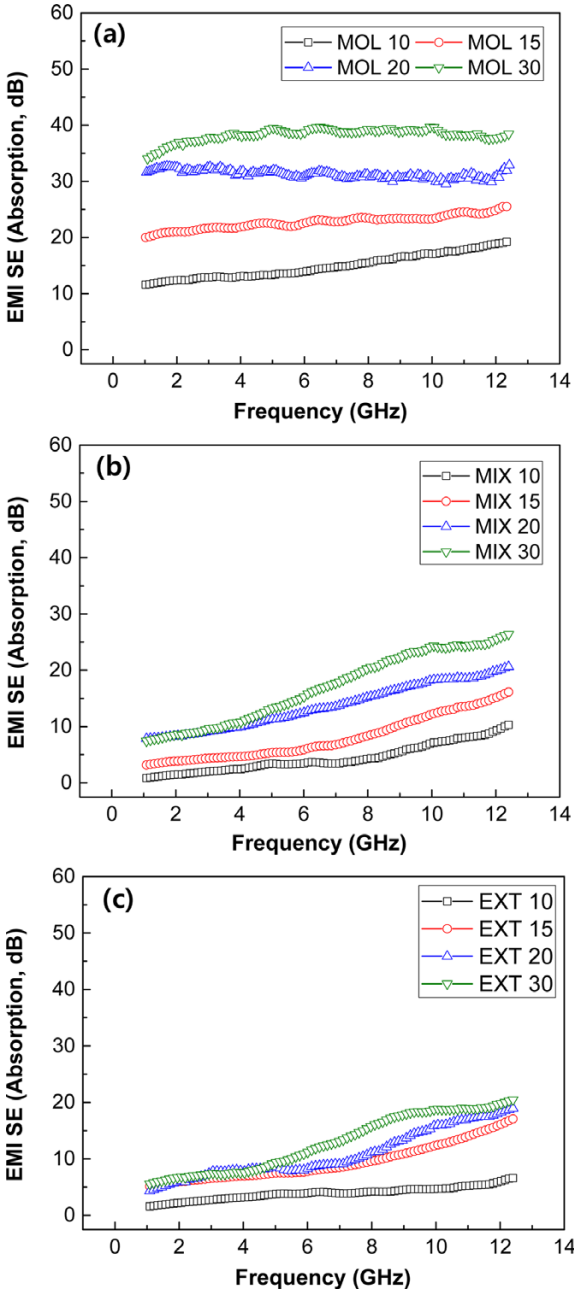

Figure 8. Absorption part of the EMI shielding effectiveness (SE_A) of the PP/CF composites with frequency and CF contents. Samples were prepared by different processing methods: (a) Injection molding, (b) internal mixing, and (c) screw extrusion.

to the value of SE_R. The results of Figures 7 and 8 show that more specifically, the total EMI shielding effectiveness (SE_T) consists of 85.1% EMI shielding effectiveness by absorption (SE_A), and 14.9% EMI shielding effectiveness by reflection (SE_R). The explanation of the shielding mechanism by reflection can be that when an incident wave strikes the surface of the shielding material, a part of the electromagnetic wave energy is reflected, due to impedance mismatching between free space and the surface of the shieling material.[46] The explanation of the shielding mechanism by absorption is that when the rest of the electromagnetic wave passes through a medium, the electromagnetic wave loses its energy, due to dielectric, magnetic, and ohmic losses. Forming electrical networks increases dielectric and ohmic losses within the shielding material, which results in improved EMI absorption values.[46]

4. Conclusions

In this study, electrical properties of the electrical conductivities, electromagnetic parameters and EMI shielding effectiveness of the PP/CF composites prepared using injection molding machine, internal mixer and screw extruder were investigated. The results of the electrical properties of the PP/CF composites show that the PP/CF composites prepared by injection molding machine revealed the highest electrical conductivity and EMI shielding effectiveness, which values were 1.75×10^1 S/cm and 48.4 dB at the frequency of 10 GHz, respectively, when the CF content was 30 wt%. These results seem mainly due to the increased CF length of the PP/CF composite when the samples were prepared by injection molding (884 μm), compared that of the composites prepared by internal mixer (613 μm) and screw extrusion (407 μm), which was advantageous in forming conductive networks of the composites.

The results of the electromagnetic parameters of the dielectric constants (ε' and ε'') and magnetic parameters (μ' and μ'') of the PP/CF composites indicate that the increased electrical conductivity of the PP/CF composites prepared by injection molding was mainly due to the increased dielectric constants of the real part (ε') and the imaginary part (ε'') of the PP/CF composite. This enhanced permittivity ($\varepsilon_r=\varepsilon'-j\varepsilon''$) seems related to the percolation at lower concentration of the CF, which was affected by the increased CF length of the composite prepared by the injection molding process.

The results of the electromagnetic absorbing mechanism by the dielectric loss factor (tan $\delta_\varepsilon=\varepsilon''/\varepsilon'$) and magnetic loss factor (tan $\delta_\mu=\mu''/\mu'$) of the PP/CF composites show that the major electromagnetic absorbing mechanism was dielectric loss, such as dipole polarization and interface polarization between filler and matrix, which resulted in improved EMI absorption values. The results of the EMI shielding effectiveness of the PP/CF composites show that the total EMI shielding effectiveness (SE_T) consisted of 85.1% EMI shielding effectiveness by absorption (SE_A), and 14.9% EMI shielding effectiveness by reflection (SE_R), which suggests that the absorbing mechanism of the incident electromagnetic wave provided the predominant EMI shielding.

References

(1) F. Shahzad, M. Alhabeb, C. B. Hatter, B. Anasori, S. M. Hong, C. M. Koo, and Y. Gogotsi, *Science,* **353**, 1137 (2016).
(2) A. H. Frey, *Health Perspect.*, **106**, 101 (1998).
(3) H. Wang, N. Ma, Z. Yan, L. Deng, J. He, Y. Hou, Y. Jiang, and G. Yu, *Nanoscale,* **7**, 7189 (2015).
(4) Q. Ling, J. Sun, Q. Zhao, and Q. Zhou, *Mater. Sci. Eng. B,* **162**, 162 (2009).
(5) N. Zhao, T. Zou, C. Shi, J. Li, and W. Guo, *Mater. Sci. Eng. B,* **127**, 207 (2006).
(6) A. Ameli, P. U. Jung, and C. B. Park, *Carbon*, **60**, 379, (2013).
(7) N. Abbas and H. T. Kim, *Macromol. Res.*, **24**, 1084 (2016).
(8) G. Salimbeygi, K. Nasouri, A. M. Shoushtari, R. Malek, and F. Mazaheri,

Macromol. Res., **23**, 741 (2015).
(9) A. Chaudhary, S. Kumari, R. Kumar, S. Teotia, B. P. Singh, A. P. Singh, S. K. Dhawan, and S. R. Dhakate, *ACS Appl. Mater. Interfaces,* **8**, 10600 (2016).
(10) M. Arjmand, T. Apperley, M. Okoniewski, and U. Sundararaj, *Carbon*, **50**, 5126 (2012).
(11) M. H. Al-Saleh, S. A. Jawad, and H. M. El Ghanem, *High Perform. Polym.,* **26**, 205 (2013).
(12) S. Kim, J. W. Lee, I.-K. Hong, and S. Lee, *Macromol. Res.,* **22**, 154 (2014).
(13) S. W. Yoon, S. Lee, I. S. Choi, Y. Do, and S. Park, *Macromol. Res.,* **23**, 713 (2015).
(14) M. Lee, J. Koo, H. Ki, K. H. Lee, B. H. Min, Y. C. Lee, and J. H. Kim, *Macromol. Res.,* **25**, 231 (2017).
(15) W. I. Jang, J. W. Lee, Y. M. Baek, and O O. Park, *Macromol. Res.,* **24**, 276 (2016).
(16) F. Shahzad, P. Kumar, Y.-H. Kim, S. M. Hong, and C. M. Koo, *ACS Appl. Mater. Interfaces,* **8**, 9361 (2016).
(17) P. Kumar, F. Shahzad, S. Yu, S. M. Hong, Y.-H. Kim, and C. M. Koo, *Carbon,* **94**, 494 (2015).
(18) J. M. Kim, D. H. Kim, J. Kim, J. W. Lee, and W. N. Kim, *Macromol. Res.,* **25**, 190 (2017).
(19) M. G. Jang, Y. K. Lee, and W. N. Kim, *Macromol. Res.*, **23**, 916 (2015).
(20) S. J. Lim, J. G. Lee, S. H. Hur, and W. N. Kim, *Macromol. Res.,* **22**, 632 (2014).
(21) S. H. Lee, E. Cho, S. H. Jeon, and J. R. Youn, *Carbon*, **45**, 2810 (2007).
(22) F. Shahzad, S. Yu, P. Kumar, J.-W. Lee, Y.-H. Kim, S. M. Hong, and C. M. Koo, *Compos. Struct.,* **133**, 1267 (2015).
(23) Y. Xu, Y. Li, W. Hua, A. Zhang, and J. Bao, *ACS Appl. Mater. Interfaces,* **8**, 24131 (2016).
(24) S. Yu, J.-W. Lee, T. H. Han, C. Park, Y. Kwon, S. M. Hong, and C. M. Koo, *ACS Appl. Mater. Interfaces,* **5**, 11618 (2013).
(25) H. B. Zhao, Z. B. Fu, H. B. Chen, M. L. Zhong, and C. Y. Wang, *ACS Appl. Mater. Interfaces,* **8**, 1468 (2016).
(26) B. Zhao, X. Guo, W. Zhao, J. Deng, G. Shao, B. Fan, Z. Bai, and R. Zhang, *ACS Appl Mater Interfaces,* **8**, 28917 (2016).
(27) J. Zeng and J. Xu, *J. Alloy Compd.*, **493**, 39 (2010).
(28) G. Shen, Z. Xu, and Y. Li, *J. Magn. Magn. Mater.,* **301**, 325 (2006).
(29) B. Qu, C. Zhu, C. Li, X. Zhang, and Y. Chen, *ACS Appl. Mater. Interfaces,* **8**, 3730 (2016).
(30) J. Liu, R. Che, H. Chen, F. Zhang, F. Xia, Q. Wu, and M. Wang, *Small*, **8**, 1214 (2012).
(31) J.-Z. He, X.-X. Wang, Y.-L. Zhang, and M.-S. Cao, *J. Mater. Chem. C,* **4**, 7130 (2016).
(32) J. Xu, J. Liu, R. Che, C. Liang, M. Cao, Y. Li, and Z. Liu, *Nanoscale*, **6**, 5782 (2014).
(33) T. W. Yoo, Y. K. Lee, S. J. Lim, H. G. Yoon, and W. N. Kim, *J. Mater. Sci.*, **49**, 1701 (2014).
(34) D. H. Park, Y. K. Lee, S. S. Park, C. S. Lee, S. H. Kim, and W. N. Kim, *Macromol. Res.,* **21**, 905 (2013).
(35) M. G. Jang, C. Cho, and W. N. Kim, *J. Compos. Mater.*, **51**, 1005 (2017).
(36) G. Lu, X. Li, and H. Jiang, *Compos. Sci. Technol.*, **56**, 193 (1996).
(37) G.-Y. Heo, Y.-T. Hong, and S.-J. Park, *Macromol. Res.*, **20**, 503 (2012).
(38) B. Yuan, L. Yu, L. Sheng, K. An, and X. Zhao, *J. Phys. D: Appl. Phys.*, **45**, 235108 (2012).
(39) C. R. Paul, *Introduction to Electromagnetic Compatibility*, 2nd ed., Wiley Interscience, Hoboken, NJ, 2006.
(40) J.-M. Thomassin, C. Jérôme, T. Pardoen, C. Bailly, I. Huynen, and C. Detrembleur, *Mater. Sci. Eng. R.-Rep.*, **74**, 211 (2013).
(41) F. Qin and C. Brosseau, *J. Appl. Phys.*, **111**, 61301 (2012).
(42) P. Pötschke, S. M. Dudkin, and I. Alig, *Polymer,* **44**, 5023 (2003).
(43) T. Nakamura, *J. Appl. Phys.*, **88**, 348 (2000).
(44) C. Wang, X. Han, P. Xu, X. Zhang, Y. Du, S. Hu, J. Wang, and X. Wang, *Appl. Phys. Lett.*, **98**, 072906 (2011).
(45) N. Li, Y. Huang, F. Du, X. He, X. Lin, H. Gao, Y. Ma, F. Li, Y. Chen, and P. C. Eklund, *Nano Lett.*, **6**, 1141 (2006).
(46) H. W. Ott, *Electromagnetic Compatibility Engineering*, Wiley, New York, 2009.

